Physica E 121 (2020) 114113

Contents lists available at ScienceDirect

Physica E: Low-dimensional Systems and Nanostructures

journal homepage: http://www.elsevier.com/locate/physe

Tailoring and probing the quantum states of matter of 2D Dirac materials with a buckled honeycomb structure

Z. Jiao, Q. Yao, H.J.W. Zandvliet *

Physics of Interfaces and Nanomaterials, MESA+ Institute for Nanotechnology, University of Twente, P.O. Box 217, 7500AE, Enschede, the Netherlands

A B S T R A C T

The quantum state of matter of a two-dimensional Dirac material with a buckled honeycomb structure can be tuned by an electric field. In the absence of an external electric field the material is a topological insulator owing to the spin-orbit coupling, which opens a band gap at the K and $K^{'}$ points of the Brillouin zone. The size of this band gap decreases with increasing electric field until eventually the band gap completely closes at a critical electric field E_c and the material becomes a semi-metal. For electric fields exceeding E_c the band gaps reopens again and the material undergoes a topological phase transition from a semi-metal to a normal band insulator.

The electric field in a tunnel junction depends on the applied voltage bias across the junction as well as the difference in work function of the two electrodes. Here we show how scanning tunneling microscopy can be employed to simultaneously apply an electric field and study the electronic structure of a two-dimensional Dirac material with a buckled honeycomb structure. The electric field applied by the scanning tunneling microscope offers the possibility to locally alter the quantum state of matter of two-dimensional topological insulator to a semi-metal or normal band insulator. This results in the development of topologically protected spin polarized edge states *within* the material. We present a spectroscopic method to probe these topologically protected edge states.

1. Introduction

The successful isolation of graphene [1,2], i.e. a single layer of sp^2 hybridized carbon atoms arranged in a honeycomb structure, has resulted into the opening of a new research field. Graphene exhibits many interesting and unique properties. Most of these properties are intimately related to the linear dispersion relation of the electrons in the vicinity of the Fermi level [3–6]. Near the K and $K^{'}$ points of the Brillouin zone the linearly dispersing energy bands lead to Dirac cones. If spin-orbit coupling is not taken into account, graphene has no band gap and a vanishing density of states at the Fermi level. If, however, spin-orbit coupling is taken into account a band gap at the K and $K^{'}$ points of the Brillouin zone is present. The spin-orbit gap in graphene is only about 20 μeV and therefore it will not be detectable at any experimentally accessible temperature [7,8].

Silicon, germanium and tin atoms have a similar electronic configuration as carbon atoms and therefore these atoms might also form a two-dimensional honeycomb lattice [9–16]. Theoretical studies have revealed that the graphene-like allotropes of silicon, germanium and tin referred to as silicene, germanene and stanene respectively, can indeed exist. These two-dimensional materials share many properties with their carbon counterpart [17–21]. For instance, the energy bands near the K and $K^{'}$ points of the Brillouin zone are linear and the charge carrier mobilities and Fermi velocities are very comparable to graphene. Unfortunately, silicene, germanene and stanene do not occur in nature and therefore these materials have to be synthesized. Silicene has been successfully synthesized in 2012, followed by germanene in 2014 [9–15] and stanene, sometimes also referred to as tinene in 2015 [22].

Silicene, germanene and stanene also exhibit some properties that are different from graphene. The most eye-catching difference with graphene is the corrugation: the honeycomb lattices of silicene, germanene and stanene are buckled [17], i.e. the two triangular sub-lattices of the honeycomb lattice are displaced with respect to each other in a direction normal to the two-dimensional layer. This buckling is caused by the relatively large, at least as compared to carbon, ionic radii of silicon, germanium and tin, which prohibits the formation of a perfectly planar honeycomb lattice. The buckling breaks the symmetry of the honeycomb lattice and offers the appealing possibility to transfer charge from one triangular sub-lattice to the other sub-lattice, for instance, the application of an external electric field [23,24]. This charge transfer results into the opening of a band gap, which paves the way to the tailoring of the quantum state of matter of these two-dimensional material as well as field-effect based device applications. Like graphene, silicene, germanene and stanene belong to the class of Z_2 topological insulators [25,26]. The spin-orbit coupling in silicene (3.9 meV), germanene (43 meV) and stanene (100 meV) results in the opening of a

* Corresponding author.
E-mail address: h.j.w.zandvliet@utwente.nl (H.J.W. Zandvliet).

https://doi.org/10.1016/j.physe.2020.114113
Received 22 August 2019; Received in revised form 18 September 2019; Accepted 22 March 2020
Available online 27 March 2020
1386-9477/© 2020 The Authors. Published by Elsevier B.V. This is an open access article under the CC BY license (http://creativecommons.org/licenses/by/4.0/).

spin-orbit band gap at the K and K' points of the Brillouin zone [27–29]. As shown by Drummond, Z'olyomi and Fal'ko [23] as well as Ezawa [24] the application of a transverse electric field first closes and then reopens the band gap. With increasing electric field silicene, germanene and stanene undergo a topological phase transition from a topological insulator to a semi-metal and subsequently to a normal band insulator [23,24,30,31]. It has been pointed out by Ezawa {24] that the application of an inhomogeneous electric field, for instance by using a scanning tunneling microscope, can result in the development of topologically protected and spin polarized edge states anywhere *within* the two-dimensional material [24].

Inspired by Ezawa's work we are dedicated to search for an experimental method to prove the existence of these topologically protected edge states within a material. The requirement of a high spatial resolution puts severe constraints and basically limits our search to scanning probe microscope-based techniques. Scanning tunneling microscopy and spectroscopy are often employed to study the structural and electronic properties of two-dimensional materials. There is, however, also a point of concern when using scanning tunneling microscopy. The voltage drop across the tunnel junction, which can be as a few Volts per nm can affect the electronic structure of the material under scrutiny. Here, however, this electric field is advantageous since it allows us to modify the electronic band structure of the buckled two-dimensional materials.

In this work we will not only study the effect of an electric field on the density of states of a buckled two-dimensional material with a honeycomb lattice, but we also put forward a method that allows to study the formation of topologically protected edge states within the material. Our method relies on the presence of topologically protected edge states at the boundary between a the two-dimensional topological insulator and a semi-metal or normal band insulator [24]. The topologically protected edge states act as barriers for incoming electron waves resulting in standing wave patterns, which will show up as peaks in the scanning tunneling spectroscopy spectra.

1.1. Quantum states of matter of buckled 2D Dirac materials

Elemental two-dimensional elemental materials such as silicene and germanene exhibit a buckled honeycomb lattice, which is composed of two triangular sub-lattices. These two triangular sub-lattices are slightly displaced with respect to each other in a direction normal to the two-dimensional sheet. The displacement or buckling is denoted by Δ. The buckling of free-standing silicene and germanene is 0.44 Å and 0.66 Å, respectively. For the sake of simplicity we consider here a perfect, i.e. defect free and impurity free, single sheet of a buckled two-dimensional elemental material. As shown in Refs. [24] the energy dispersion in the vicinity of the K and K' points of the Brillouin zone is given by,

$$E_{\pm} = \pm\sqrt{\hbar^2 v_F^2 k^2 + \left(\frac{\Delta}{2} eE_z - \zeta s\lambda_{SO}\right)^2} \tag{1}$$

where $\zeta = \pm 1$ refers to the K (K') point, $s = \pm 1$ to the spin, E_z to the electric field, e to the unit of elementary charge, λ_{SO} to the spin-orbit gap, v_F to the Fermi velocity, k to the momentum and $\hbar$ to the reduced Planck's constant. For a vanishing spin-orbit coupling and electric field the well-known Dirac cones are recovered, i.e. $E_{\pm} = \pm \hbar v_F k$. We would like to emphasize here that this method is not applicable to graphene owing to its planar structure, which prohibits the transfer of charge from one sub-lattice to the other sub-lattice.

The electric field E_z can have different contributions. For instance, in a scanning tunneling microscope junction the electric field has in general two components. The first component is caused by the applied sample bias, V, resulting in an electric field $\frac{V}{d}$, where d is the tip-sample distance. The second component is due to a difference in work function between tip and substrate. This difference in work function, $\delta W = W_t - W_s$, results in an electric field $(\delta W/e)/(d)$. The total electric field, E_z, in the tunnel junction is then given by $(V + \delta W/e)/d$.

For completeness we also include a Rashba coupling, λ_R, but as we will see later the Rashba coupling has no effect on the actual size of the band gap at the Dirac points [24,30]. The full expression of the dispersion relations in the vicinity of the K point that includes a spin-orbit coupling, an electric field and a Rashba coupling is given by,

$$E_{\pm} = \pm\sqrt{\hbar^2 v_F^2 k^2 + \left(\frac{\Delta}{2}\left(\frac{eV + \delta W}{d}\right) - \zeta s\sqrt{\left(\lambda_{SO}^2 + \alpha^2\lambda_R^2 k^2\right)}\right)^2} \tag{2}$$

where α is a constant. Please note that Eq. (2) reduces to Eq. (1) at the Dirac points, i.e. at $k = 0$. In Fig. 1 we show an overview of the different topological quantum states of matter of a two-dimensional Dirac material with a buckled honeycomb lattice. For a vanishing electric field the material is a two-dimensional topological insulator (left panel). In the middle panel the applied electric field is just large enough to close the spin-orbit gap for the spin up and spin down bands at the K and K' points, respectively. At this condition the material behaves as a perfect semi-metal. For electric fields that exceeds the spin-orbit gap, the band gap reopens again and the material becomes a normal band insulator.

At $k = 0$ we find in principle two branches with a band gap,

$$E_{gap} = 2\left|\frac{\Delta}{2} eE_z - \zeta s\lambda_{SO}\right| \tag{3}$$

where $\zeta s = \pm 1$. The band gap closes at the critical electric field $E_c \pm \frac{2}{\Delta e}\lambda_{SO}$. The critical fields for silicene and germanene are ± 0.18 V/nm and ± 1.3 V/nm, respectively. In Fig. 2 a schematic figure of the energy bands at the K point versus the electric field is depicted.

An ideal technique to explore the effect of an electric field on the quantum state of matter is scanning tunneling microscopy. The density of states can be obtained by recording a current (I)- voltage (V) trace at constant tip-sample distance. The differential conductivity (dI/dV) is proportional to the density of states. Since the electric field in the tunneling junction also depends on the tip-sample bias we have to disentangle this effect from the measured density of states. For the sake of simplicity we consider here the case that the work function difference between tip and substrate, which results in an offset of the electric field, is zero. In the absence of an electric field, i.e. $E_z = 0$, the density of states, $D(E)$, of both spin branches at the K point are given by,

$$D(E) = \frac{D(k)2\pi k dk}{\left(\frac{dE}{dk}\right)} = \frac{|E - \lambda_{SO}|}{2\pi\hbar^2 v_F^2} \tag{4a}$$

The total density of states at energy E is then (K and K' points and two spin bands),

$$D(E) = \frac{2|E - \lambda_{SO}|}{\pi\hbar^2 v_F^2} \tag{4b}$$

For an applied electric field, E_z, the spin up and spin down gaps at the K point are given by,

$$E_{g,s=+1} = 2\left|\frac{\Delta}{2} eE_z - \lambda_{SO}\right| \tag{5a}$$

and

$$E_{g,s=-1} = 2\left|\frac{\Delta}{2} eE_z + \lambda_{SO}\right|, \tag{5b}$$

Similar expressions can be derived for the K' point. The only difference is the sign in front of the λ_{SO} term. Here we restrict ourselves to (1) the E_+ branch at the K point and (2) positive electric fields, i.e. $E_z > 0$. The application of a voltage, V, across the scanning tunneling microscopy junction results in an electric field $\frac{V}{d}$, which will lead to charge transfer from one triangular sub-lattice to the other triangular sub-lattice. This charge transfer will lead to an increase (decrease) of the band gap of the spin up (down) band. From a scanning tunneling

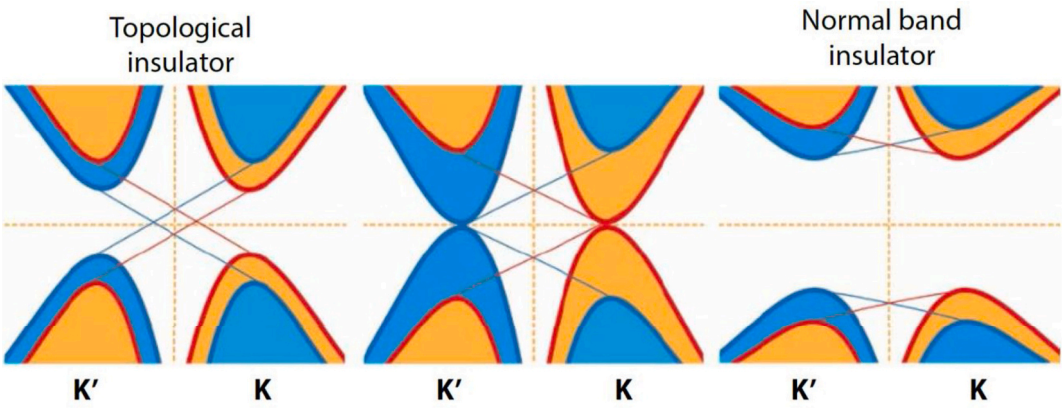

Fig. 1. Schematic cartoon of the electronic band structure of a two-dimensional Dirac material with a buckled honeycomb lattice. Left panel: electric field smaller than spin-orbit gap. The material is a topological insulator. Middle panel: electric field is equal to spin-orbit gap. The material is a semi-metal. Right panel: electric field is larger than spin-orbit gap. The material is a normal band insulator. Blue: spin down bands. Orange: spin up bands. (For interpretation of the references to colour in this figure legend, the reader is referred to the Web version of this article.)

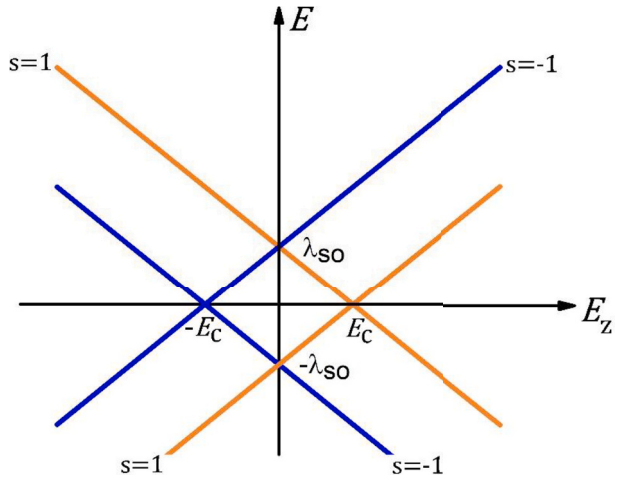

Fig. 2. The energy bands at the K point of the Brillouin zone versus electric field. Blue: spin down bands. Orange: spin up bands. (For interpretation of the references to colour in this figure legend, the reader is referred to the Web version of this article.)

spectroscopy measurement one can extract the exact location of these two band gaps. The first gap is found that a threshold voltage V_1,

$$eV_1 = \lambda_{SO} - \frac{e\Delta}{2d}V_1 \tag{6a}$$

In the density of states a kink will be found when the second spin band comes into play. The second gap has a threshold voltage V_2,

$$eV_2 = \lambda_{SO} + \frac{e\Delta}{2d}V_2 \tag{6b}$$

The density of states can be found by simply adding up the two spin bands and multiply with a factor of two due to the two different K points. The total density of states is then given by,

$$D(E) = 0 \quad \text{for} \quad 0 \le eV \le \frac{\lambda_{SO}}{\left(1+\frac{\Delta}{2d}\right)} \tag{7a}$$

$$D(E) = \frac{eV\left(1+\frac{\Delta}{2d}\right) - \lambda_{SO}}{\pi\hbar^2 v_F^2} \quad \text{for} \quad \frac{\lambda_{SO}}{\left(1+\frac{\Delta}{2d}\right)} \le eV \le \frac{\lambda_{SO}}{\left(1-\frac{\Delta}{2d}\right)} \tag{7b}$$

$$D(E) = \frac{2(eV-\lambda_{SO})}{\pi\hbar^2 v_F^2} \quad \text{for} \quad \frac{\lambda_{SO}}{\left(1-\frac{\Delta}{2d}\right)} \le eV \le \frac{2d\lambda_{SO}}{\Delta} \tag{7c}$$

$$D(E) = \frac{2eV\left(1-\frac{\Delta}{2d}\right)}{\pi\hbar^2 v_F^2} \quad \text{for} \quad eV \ge \frac{2d\lambda_{SO}}{\Delta} \tag{7d}$$

Similar expressions can be found for negative sample biases. Usually the tunneling current is dominated by electronic states at the Γ point of the surface Brillouin zone, since this results in the smallest inverse decay length [32]. However, if there are no states available at the Γ point tunneling will occur to, or from, electronic states with a non-zero parallel momentum [32]. In the vicinity of the Fermi level of two-dimensional elemental materials, such as graphene, silicene and germanene, there are only electronic states at the K and K' points of the Brillouin zone and therefore the density of states only comes from these k-points.

We now return to equations (7a)-(d) to discuss the impact of the electric field of the scanning tunneling microscopy junction on the density of states. The slope of the density of states changes with increasing energy from 0 to $\left(1+\frac{\Delta}{2d}\right)$ to 2 and finally to $2\left(1-\frac{\Delta}{2d}\right)$. Since $d \gg \Delta$ ($\frac{\Delta}{2d}$ is about 0.022 for silicene and 0.033 for germanene) the most pronounced change in the density of states occurs at $eV \approx \lambda_{SO}$.

Let's assume that we set the electric field to a value larger than its critical value, i.e. $E_c = \frac{2\lambda_{SO}}{e\Delta}$, which implies that the circular region underneath the tip has become a normal band insulator (see Fig. 3). For the sake of simplicity we consider the STM tip as a simple rod with radius R. The interface between the small circular shaped band insulator with radius R and the surrounding topological insulator host will act as a barrier for incoming electron waves leading to an electron interference pattern. For simplicity we reduce this problem to that of a quantum mechanical particle trapped in an infinitely deep circular well with a radius R. A few remarks are in place here: (1) in reality the transition from a normal band insulator to a the two-dimensional topological insulator leads a barrier of finite height, where the incoming electrons are scattered and (2) we assume that the electrons at the bottom of conduction have a parabolic dispersion relation with an effective mass m_{eff}. The eigenfunctions and energy eigenvalues are given by,

$$\psi(r,\theta) = CJ_m\left(\frac{z_{m,n}}{R}r\right)e^{ima} \tag{8a}$$

and

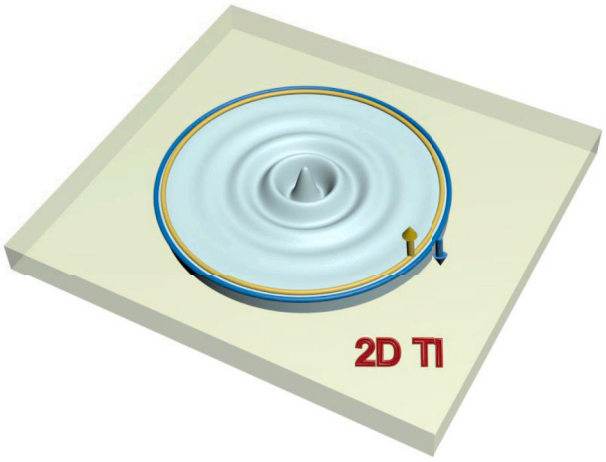

Fig. 3. Schematic picture of the development of topologically protected helical zero modes due to the electric field of a scanning tunneling microscope. Underneath the scanning tunneling microscope tip the quantum state of matter can be changed from a two-dimensional topological insulator to a normal band gap insulator. The electron standing wave pattern results in resonances in the z (V) signal.

$$E_{m,n} = \frac{\hbar^2}{2m_{eff}} \left(\frac{z_{m,n}}{R}\right)^2 \tag{8b}$$

where r and θ are the polar coordinates, C a constant, J_m the Bessel function of the first kind and order m, $m \in \mathbb{Z}$, $n \in \mathbb{N}$ and $z_{m,n}$ the nth zero of the Bessel function of the first kind and order m. For instance for $m = 0$ the first 4 zeros are given by 2.4048, 5.5207, 8.6537 and 11.7915 respectively [33]. For $m = 0$ these electron standing waves patterns will exhibit a strong maximum in the middle of the circle, i.e. precisely at the location of the scanning tunneling microscope tip, see Fig. 3. If we record the z-piezo displacement versus sample bias, i.e. $z(V)$, at constant tunnel current we will find a resonance in the $z(V)$ signal if a standing wave pattern occurs. The $z(V)$ signal provides direct information on the position of the energy eigenvalues of this system [34–36]. However, more important is the fact that the presence of these electron standing waves implies that we must have formed topologically protected edges state within the material.

For electric fields exceeding the critical field the region just underneath the scanning tunneling microscope tip will become a normal band insulator. Since the energy of tunneling electrons is higher (lower) than the minimum (maximum) of the conduction (valence band) and therefore we expect also in this case the development of electron standing waves patterns. In order to avoid field emission resonances, which can occur at voltages exceeding the work function of the substrate, it is advisable to keep the maximum voltage in the $z(V)$ measurement below the work function of the substrate.

2. Conclusions

The quantum state of matter of a two-dimensional Dirac material with a buckled honeycomb lattice can be tuned from a topological insulator to a semimetal or a normal band insulator by applying an external electric field. The application of a spatially inhomogeneous electric field, by for instance an STM, allows to *locally* change the quantum state of matter. The STM can simultaneously be used to probe the changes in electronic structure upon the application of an electric field. Here we show how the electric field of the scanning tunneling microscope affects the electronic structure of a buckled two-dimensional Dirac material. In addition, we have proposed a method, that relies on $z(V)$ spectroscopy, to obtain more information on the presence of topologically protected edge states within the material.

Declaration of competing interest

There is no conflict of interest regarding this manuscript.

Acknowledgements

Q.Y. and Z.J. thank the China Scholarship Council for financial support. H.J.W.Z. acknowledges the Nederlandse organisatie voor Wetenschappelijk Onderzoek (NWO) for financial support.

References

[1] K.S. Novoselov, A.K. Geim, S.V. Morozov, D. Jiang, Y. Zhang, S.V. Dubonos, I. V. Grigorieva, A.A. Firsov, Science 306 (2004) 666.
[2] A.K. Geim, K.S. Novoselov, Nat. Mater. 6 (2007) 183.
[3] A.H. Castro Neto, F. Guinea, N.M.R. Peres, K.S. Novoselov, A.K. Geim, Rev. Mod. Phys. 81 (2009) 109.
[4] S. Das Sarma, S. Adam, E.H. Hwang, E. Rossi, Rev. Mod. Phys. 83 (2011) 407.
[5] M.O. Goerbig, Rev. Mod. Phys. 83 (2011) 1193.
[6] V.N. Kotov, B. Uchoa, V.M. Pereira, F. Guinea, A.H. Castro Neto, Rev. Mod. Phys. 84 (2012) 1067.
[7] H. Min, J.E. Hill, N.A. Sinitsyn, B.R. Sahu, L. Kleinman, A.H. MacDonald, Phys. Rev. B 74 (2006), 165310.
[8] Y. Yao, F. Ye, X.-L. Qi, S.-C. Zhang, Z. Fang, Phys. Rev. B 75 (2007), 041401.
[9] P. Vogt, P. De Padova, C. Quaresima, J. Avila, E. Frantzeskakis, M.C. Asensio, A. Resta, B. Ealet, G. Le Lay, Phys. Rev. Lett. 108 (2012), 155501.
[10] A. Fleurence, R. Friedlein, T. Ozaki, H. Kawai, Y. Wang, Y. Yamada-Takamura, Phys. Rev. Lett. 108 (2012), 245501.
[11] L. Li, S.-Z. Lu, J. Pan, Z. Qin, Y.-Q. Wang, Y. Wang, G. Cao, S. Du ad, H.-J. Gao, Adv. Mater. 26 (2014) 4820.
[12] M.E. Dávila, L. Xian, S. Cahangirov, A. Rubio, G. Le Lay, New J. Phys. 16 (2014), 095002.
[13] P. Bampoulis, L. Zhang, A. Safaei, R. van Gastel, B. Poelsema, H.J.W. Zandvliet, J. Phys. Condens. Matter 26 (2014), 442001.
[14] L. Zhang, P. Bampoulis, A. van Houselt, H.J.W. Zandvliet, Appl. Phys. Lett. 107 (2015) 111605.
[15] L. Zhang, P. Bampoulis, A.N. Rudenko, Q. Yao, A. van Houselt, B. Poelsema, M. I. Katsnelson, H.J.W. Zandvliet, Phys. Rev. Lett. 116 (2016), 256804.
[16] M. Ezawa, J. Phys. Soc. Jpn. 84 (2015), 121003.
[17] K. Takeda, K. Shiraishi, Phys. Rev. B 50 (1994) 14916.
[18] G.G. Guzmán-Verri, L.C. Lew Yan Voon, Phys. Rev. B 76 (2007), 075131.
[19] S. Cahangirov, M. Topsakal, E. Aktürk, H. Şahin, S. Ciraci, Phys. Rev. Lett. 102 (2009), 236804.
[20] A. Molle, et al., Nat. Mater. 16 (2017) 163.
[21] A. Acun, et al., J. Phys. Condens. Matter 27 (2015) 443002.
[22] F.-F. Zhu, W.-J. Chen, Y. Xu, C.-L. Gao, D.-D. Guan, C.-H. Liu, D. Qian, S.-C. Zhang, J.-F. Jia, Nat. Mater. 14 (2015) 1020.
[23] N.D. Drummond, V. Zólyomi, V.I. Fal'ko, Phys. Rev. B 85 (2012), 075423.
[24] M. Ezawa, New J. Phys. 14 (2012), 033003.
[25] C.L. Kane, E.J. Mele, Phys. Rev. Lett. 95 (2005), 146802.
[26] C.L. Kane, E.J. Mele, Phys. Rev. Lett. 95 (2005), 226801.
[27] C.-C. Liu, W. Feng, Y. Yao, Phys. Rev. Lett. 107 (2011), 076802.
[28] Y. Xu, et al., Phys. Rev. Lett. 111 (2013) 136804.
[29] C.-C. Liu, H. Jiang, Y. Yao, Phys. Rev. B 84 (2011), 195430.
[30] M. Ezawa, Eur. Phys. J. B 86 (2012) 139.
[31] M. Ezawa, New J. Phys. 16 (2014), 065015.
[32] J.A. Stroscio, R.M. Feenstra, A.P. Fein, Phys. Rev. Lett. 57 (1986) 2579.
[33] C.W. David, Chem. Edu. Mater. 12 (2006).
[34] A. Pronschinske, D.J. Mardit, D.B. Dougherty, Phys. Rev. B 84 (2011), 205427.
[35] M. Ziegler, N. Néel, A. Sperl, J. Kröger, R. Berndt, Phys. Rev. B 80 (2009), 125402.
[36] C. Hellenthal, R. Heimbuch, K. Sotthewes, E.S. Kooij, H.J.W. Zandvliet, Phys. Rev. B 88 (2013), 035425.